Uniaxial planar deformation of PET films: 2. Characterization of the orientation from measurements of refractive indices

P. Lapersonne
Rhône Poulenc Recherches, Centre de Recherches des Carrières, 85 Av. des Frères Perret, BP 62, 69192 Saint Fons Cedex, France

and J. F. Tassin*
Université du Maine, Laboratoire de PhysicoChimie Macromoléculaire, Unité Associée au CNRS no. 509, Av. Olivier Messiaen, 72017 Le Mans Cedex, France

and L. Monnerie
Ecole Supérieure de Physique et Chimie de Paris, Laboratoire de PhysicoChimie Structurale et Macromoléculaire, Unité Associée au CNRS no. 278, 10 rue Vauquelin, 75231 Paris Cedex 05, France
(Received 8 April 1993; revised 21 July 1993)

Refractive indices along the three principal directions of uniaxial planar deformed poly(ethylene terephthalate) (PET) films have been used to calculate the second moments of the orientation distribution of the phenyl ring's normal with respect to the three principal directions of the sample. Under our stretching conditions, the phenyl rings show a strong tendency to orient their plane parallel to the plane of the films. The orientation of the chain axis can also be evaluated from the same data. A good correlation is observed between this indirect measurement and direct, but more tedious, techniques such as infra-red dichroism.

(Keywords: biaxial orientation; refractive indices; PET films)

INTRODUCTION

A knowledge of the molecular structure and molecular orientation is of primary importance in order to understand, and thereby control and improve, the influence of processing conditions on the final properties of a flat film. Measurement of refractive indices is among the easiest experiments to perform and can afford interesting information concerning the orientation[1]. Under uniaxial stretching conditions, the interpretation of such measurements in terms of orientation functions is well documented; however, under biaxial symmetry the situation is more complex. Attempts to correlate quantitatively refractive indices with orientation functions have been made, for example, by Stein for polyethylene[2,3]. White and Spruiell[4–7] have defined new orientation functions that can be calculated in a straightforward manner from birefringence data, if the polarizability tensor possesses uniaxial symmetry around the chain axis. Ward and co-workers[8–10] have also made qualitative use of birefringence measurements in order to characterize bioriented samples. However, quantitative deductions require further measurements to be made by other spectroscopic techniques, such as Raman scattering or infra-red dichroism.

We present here an easy method to determine orientation averages under biaxial symmetry conditions, from the refractive indices alone, in the special case of poly(ethylene terephthalate) (PET) films.

The samples used to test this method are the same as those of previous studies where the crystalline orientation was characterized by X-ray diffraction methods[11] and amorphous orientation by infra-red and Raman spectroscopy[12,13].

We first show how to characterize the biaxial orientation from refractive indices alone, then make use of this method to discuss the average orientation in uniaxial planar deformed PET films.

DETERMINATION OF BIAXIAL ORIENTATION FROM MEASUREMENTS OF REFRACTIVE INDICES

Definition of reference systems

The orthogonal reference axes fixed in the sample, $OX_1X_2X_3$, are defined with OX_1 along the draw direction and OX_2 in the plane of the film. The principal axes of the polarizability tensor are defined as $Ox_1^c x_2^c x_3^c$, such that Ox_1^c lies along the chain axis direction, Ox_2^c is perpendicular to Ox_1^c and in the plane of the terephthalic residue, and the third principal direction, Ox_3^c, is almost parallel to the phenyl ring normal (the angle between the

* To whom correspondence should be addressed

0032-3861/94/10/2192–05

two directions being 5° in the crystalline unit cell described by Daubeny *et al.*[14]).

Calculation of orientation from polarizabilities

The material will be considered as an aggregate of elementary unit cells of orthorhombic symmetry from the point of view of the polarizabilities.

Let us design by α_i the polarizability of the elementary cell with respect to the principal axis Ox_i^c. The macroscopic polarizability ϕ_i is related to the refractive index n_i along the OX_i direction of the sample by a Lorentz–Lorenz relation:

$$\phi_i = \frac{n_i^2 - 1}{n_i^2 + 2} \tag{1}$$

By means of a calculation similar to that in ref. 8, the quantities ϕ_i (where $i = 1$, 2 or 3) in the direction OX_i of the sample can be related to the properties of the polarizability tensor and to the orientation of this tensor by:

$$\frac{2\phi_3 - \phi_2 - \phi_1}{\phi_1 + \phi_2 + \phi_3} = \frac{2\Delta\alpha^e}{3\alpha_0} P_{200}^{x_3^c/X_3} + 2\frac{\delta\alpha^e}{\alpha_0} P_{202}^{x_3^c/X_3} \tag{2}$$

$$\frac{\phi_1 - \phi_2}{\phi_1 + \phi_2 + \phi_3} = \frac{4\Delta\alpha^e}{3\alpha_0} P_{220}^{x_3^c/X_3} + \frac{2}{3}\frac{\delta\alpha^e}{\alpha_0} P_{222}^{x_3^c/X_3} \tag{3}$$

where $P_{2mn}^{x_3^c/X_3}$ is a second moment average of the distribution function of the Ox_3^c with respect to the OX_3 reference axis[15], and:

$$\Delta\alpha^e = \alpha_3 - \frac{\alpha_1 + \alpha_2}{2} \tag{4}$$

$$\delta\alpha^e = \alpha_1 - \alpha_2 \tag{5}$$

$$\alpha_0 = \tfrac{1}{3}(\alpha_1 + \alpha_2 + \alpha_3) \tag{6}$$

In the case of PET, the three polarizabilities along the principal directions have been calculated[8–10,16]. Their values are presented in *Table 1*. It can be seen that α_1 and α_2 are almost equal (within 5%), whereas α_3 is lower than these two values by a factor of ~ 2. Therefore we can state, as a first approximation, that $\delta\alpha^e = 0$, which is equivalent to saying that the elementary unit cell possesses a uniaxial symmetry with respect to the x_3^c axis. Under these conditions, equations (2) and (3) can be simplified, yielding $P_{200}^{x_3^c/X_3}$ and $P_{220}^{x_3^c/X_3}$ from the measurements of n_1, n_2 and n_3, $P_{200}^{x_3^c/X_3}$ and $P_{220}^{x_3^c/X_3}$ being defined as follows:

$$P_{200}^{x_3^c/X_3} = \tfrac{1}{2}\langle 3\cos^2\theta_{x_3^c/X_3} - 1\rangle \tag{7}$$

where $\theta_{x_3^c/X_3}$ is the angle between the X_3 and x_3^c directions, and:

$$P_{220}^{x_3^c/X_3} = \tfrac{1}{6}(P_{200}^{x_3^c/X_1} - P_{200}^{x_3^c/X_2}) \tag{8}$$

$P_{200}^{x_3^c/X_3}$ characterizes the orientation of the normal to the benzene ring with respect to the plane of the film, and $P_{220}^{x_3^c/X_3}$ yields information about the orientation of x_3^c in the plane of the film, a negative value being related to a preferential orientation of the plane of the ring parallel to the stretching direction X_1. Of course, this orientation measured from refractive indices represents an average over the crystalline and amorphous phases.

Strictly speaking, *Table 1* shows that $\delta\alpha^e \neq 0$. Our calculation, however, remains valid if the first term on the right-hand side of equation (2) is much larger than the second term, i.e. if:

$$\frac{2\Delta\alpha^e}{3\alpha_0} P_{200}^{x_3^c/X_3} \gg 2\frac{\delta\alpha^e}{\alpha_0} P_{202}^{x_3^c/X_3} \tag{9}$$

The prefactors in front of the orientation functions have been reported in *Table 1*. $P_{202}^{x_3^c/X_3}$ cannot be measured directly, but can be related to other orientation functions by[8]:

$$P_{202}^{x_3^c/X_3} = \tfrac{1}{6}(2P_{200}^{x_3^c/X_3} + P_{200}^{x_3^c/X_3}) \tag{10}$$

These orientation functions have been determined previously on several samples using infra-red dichroism and Raman spectroscopy[12,13]. $|P_{202}^{x_3^c/X_3}|$ is always much lower than $P_{200}^{x_3^c/X_3}$. The highest ratio between these two terms is less than 0.1. The largest error (up to 14%) is introduced if the polarizabilities of model B are used. The other values of the polarizabilities lead to errors of less than 3%. Moreover, the sign of $P_{202}^{x_3^c/X_3}$ is not constant, in such a way that the orientation is not systematically over- or underestimated. Therefore the second term of equation (2) can be neglected with a very good approximation and the assumption of uniaxial symmetry of the principal polarizabilities is valid. In the present work, we chose $\alpha_3 = 1.20$ and $\alpha_1 = \alpha_2 = 2.21$, and the following simplified relations can be used:

$$\frac{2\phi_3 - \phi_2 - \phi_1}{\phi_1 + \phi_2 + \phi_3} = -0.36\, P_{200}^{x_3^c/X_3} \tag{11}$$

$$\frac{\phi_1 - \phi_2}{\phi_1 + \phi_2 + \phi_3} = -0.72\, P_{220}^{x_3^c/X_3} \tag{12}$$

Calculation of orientation from refractive indices

An alternative and easier method can be used in the case of uniaxial symmetry of the refractive index elementary cell, which is the case for PET[17]. Let us call $n_\parallel$ and $n_\perp$ the principal refractive indices of the elementary unit cell (in the case of PET, the parallel direction is Ox_3^c). The orientation of the elementary unit cell with respect to any reference axis fixed in the sample can be calculated assuming the additivity of the

Table 1 Polarizabilities of the PET repeat unit and evaluation of prefactors of the orientation functions

α_1 (10^{23} cm^3)	α_2 (10^{23} cm^3)	α_3 (10^{23} cm^3)	$2\Delta\alpha^e/3\alpha_0$	$2\delta\alpha^e/\alpha_0$	Reference
2.20	2.18	1.18	−0.363	0.022	9
2.26	2.16	1.20	−0.359	0.107	8, 10, 18 (model A)
2.28	1.95	1.37	−0.266	0.353	8, 10, 18 (model B)
2.22	2.13	1.22	−0.343	0.097	16

elementary refractive indices. It can easily be shown that:

$$n_3 - \frac{n_2+n_1}{2} = (n_\parallel - n_\perp) P_{200}^{x_3^c/X_3} \quad (13)$$

$$n_2 - \frac{n_3+n_1}{2} = (n_\parallel - n_\perp) P_{200}^{x_3^c/X_2} \quad (14)$$

$$n_1 - \frac{n_3+n_2}{2} = (n_\parallel - n_\perp) P_{200}^{x_3^c/X_1} \quad (15)$$

Combining the two last equations with equation (8) leads to:

$$n_1 - n_2 = 4\, P_{220}^{x_3^c/X_3} (n_\parallel - n_\perp) \quad (16)$$

Therefore two second-moment averages of the orientation distribution function can be determined from measurements of refractive indices along the three principal directions of the film. Hereafter we choose $n_\parallel = 1.372$ and $n_\perp = 1.787$, according to Kaito *et al.*[17].

Figure 1 shows a comparison between these two different ways of calculating $P_{200}^{x_3^c/X_3}$ from the measured refractive indices on a large number of PET samples, the origin of which is described later in this paper. The assumption of additivity of refractive indices of the elementary unit cells underestimates the orientation by 5% as compared with the other, more rigorous, method. For simplicity, and in view of the small differences, only the second method has been used to evaluate $P_{200}^{x_3^c/X_3}$ and $P_{220}^{x_3^c/X_3}$.

The orientation of the phenyl ring's normal can also be obtained from polarized infra-red absorption measurements in the vicinity of 875 cm^{-1}, which can be attributed to an out-of-plane deformation mode of the phenyl ring, the transition moment of which is perpendicular to the plane of the phenyl residue[16,18,19]. *Figure 2* compares the quantity $P_{200}^{x_3^c/X_3}$ calculated by the two techniques for fibres[20], uniaxially[18] or biaxially[8,21] deformed films. A satisfactory agreement is observed.

EXPERIMENTAL

Samples

Deformed PET films were obtained by a method[22,23] that is essentially equivalent to uniaxial planar (at constant width) deformation. The amorphous films were subjected to constant load at temperatures slightly above

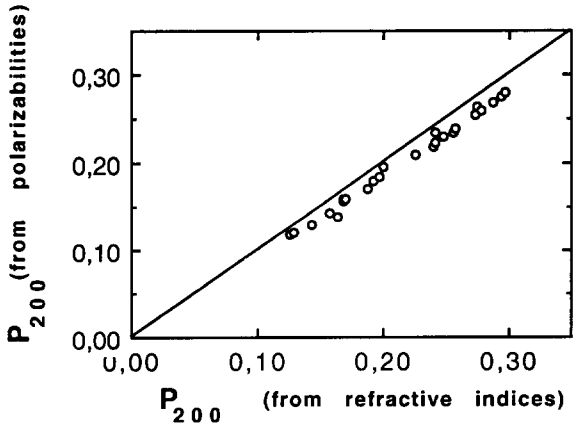

Figure 1 Comparison between $P_{200}^{x_3^c/X_3}$ calculated from polarizabilities, using equations (11) and (12), or from refractive indices directly, using equations (13)–(15)

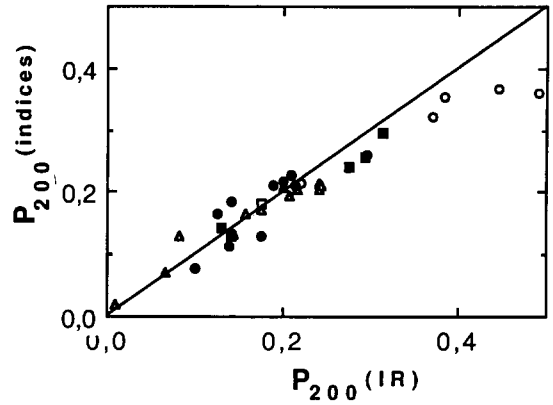

Figure 2 Comparison between $P_{200}^{x_3^c/X_3}$ calculated from measurements of refractive indices or from infra-red dichroism data: □, ref. 8; ○, ref. 21; △, ref. 18; ●, ref. 20; ■, this work

the glass transition temperature (T_g at 1 Hz ≈ 80°C). Stress-induced crystallization led to the appearance of a crystalline network which was able to equilibrate under the applied stress. The samples described in this paper were drawn with a 'short plateau' (i.e. were quenched just as they reach their equilibrium deformation under a given load and temperature). Temperature was in the range 85–110°C and the stress was varied between 2.5 and 5.52 MPa, yielding deformation ratios from 3.4 to 5.4. These samples have already been characterized from the point of view of the crystalline phase[11] (crystallinity directly related to the plateau draw ratio and increasing from 10 to 30% with the draw ratio) and a detailed study involving infra-red[13] and Raman[12] spectroscopies has been reported.

Measurement of refractive indices

An Abbe refractometer under polarized white light was used to measure the refractive indices along the three principal directions of the film, with an uncertainty of less than 1%. The refractive indices afford information about the orientation averaged over the amorphous and the crystalline phases.

RESULTS

Using measurements of refractive indices and expressions (13)–(15), the following averages of the orientation distribution function have been obtained: $P_{200}^{x_3^c/X_1}$, $P_{200}^{x_3^c/X_2}$, $P_{200}^{x_3^c/X_3}$.

The typical evolution of these three averages with the applied load, at a temperature of 90°C, is reported in *Figure 3*. As the stress increases, the three quantities show a distinct behaviour. A decrease of $P_{200}^{x_3^c/X_1}$ is observed as the stress increases. This reflects the usual fact that the chain axes, and thereby the C_1–C_4 axis of the phenyl rings, orient towards the stretching direction so that a normal direction orients perpendicularly. The minimum limiting value of $P_{200}^{x_3^c/X_1}$ would thus be -0.5.

The behaviours of $P_{200}^{x_3^c/X_2}$ and $P_{200}^{x_3^c/X_3}$ are less trivial. In the case of uniaxial drawing, one would expect the following relation between these quantities:

$$P_{200}^{x_3^c/X_2} = P_{200}^{x_3^c/X_3} = -1/2\; P_{200}^{x_3^c/X_1}$$

This has been successfully checked for uniaxially drawn PET samples. Here, $P_{200}^{x_3^c/X_2}$ and $P_{200}^{x_3^c/X_3}$ behave differently. A noticeable increase of $P_{200}^{x_3^c/X_3}$ with the stress is observed,

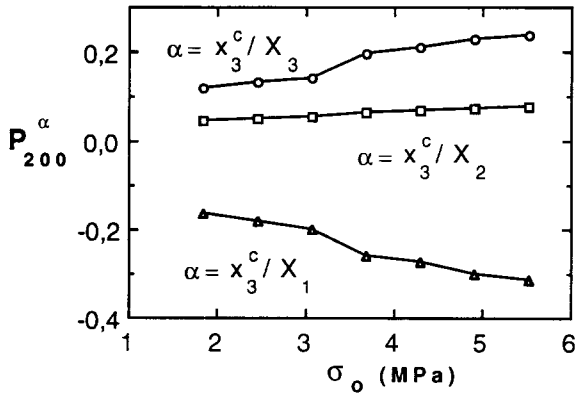

Figure 3 Phenyl ring's normal orientation with respect to directions X_1, X_2, X_3 as a function of the applied stress at 90°C

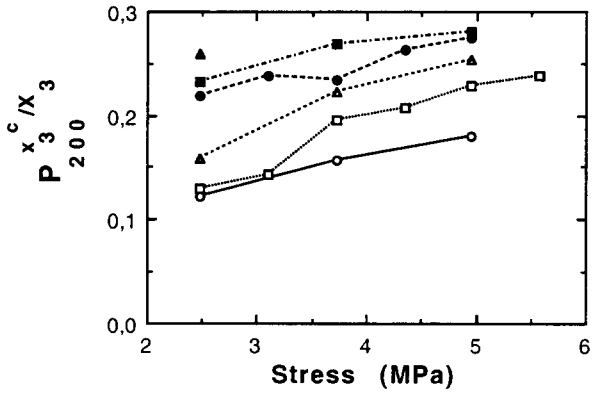

Figure 4 $P_{200}^{x_3^c/X_3}$ as a function of applied stress for various temperatures: ○, 85°C; □, 90°C; △, 95°C; ●, 100°C; ■, 105°C; ▲, 110°C

whereas $P_{200}^{x_3^c/X_2}$ remains very low (0.05–0.1) and is not greatly affected by the deformation. The fact that the difference $P_{200}^{x_3^c/X_3} - P_{200}^{x_3^c/X_2}$ increases with stress indicates a tendency of the phenyl ring to lie in the plane of the film. A similar variation of these three orientation moment averages with the applied load is obtained at other temperatures.

The $P_{200}^{x_3^c/X_3}$ data at different temperatures are plotted as a function of the applied stress in *Figure 4*. Since the $P_{200}^{x_3^c/X_2}$ values remain approximately constant (close to zero) and since $P_{200}^{x_3^c/X_1} + P_{200}^{x_3^c/X_2} + P_{200}^{x_3^c/X_3} = 0$, the tendency of the phenyl ring to lie in the plane of the film increases with temperature.

Our study on the characterization of the crystalline phase[11] has shown that the orientation of the (100) plane normals, approximately parallel to the phenyl ring normals, shows a unique relationship with the equilibrium draw ratio, λ_p, for these samples. As mentioned before, the refractive indices afford information averaged over the amorphous and crystalline phases.

Figure 5a shows the evolution of $P_{200}^{x_3^c/X_3}$ with λ_p. This macroscopic parameter affords a convenient rescaling for the orientation of the normal to the phenyl rings with respect to the thickness direction averaged over the two phases. This is not the case for $P_{220}^{x_3^c/X_3}$, as shown in *Figure 5b*, where two domains of temperature are apparent. Since $P_{220}^{x_3^c/X_3}$ is proportional to the difference between $P_{200}^{x_3^c/X_1}$ and $P_{200}^{x_3^c/X_2}$, and since this last quantity remains in absolute value less than the first one and shows a weak variation with the draw ratio, this behaviour must be attributed mainly to the evolution of $P_{200}^{x_3^c/X_1}$. This orientation moment average is plotted *versus* λ_p in *Figure 6*. At the lowest temperatures (between 85 and 95°C) a decrease of $P_{200}^{x_3^c/X_1}$ with the draw ratio is observed. Between 95 and 100°C, a relaxation phenomenon can be observed. Above 100°C the orientation increases with increasing draw ratio in a way that seems fairly independent of the temperature. The origin of this relaxation process can be attributed to the chain axes in the amorphous phase, especially to their orientation before stress-induced crystallization. More details will be provided in a forthcoming paper, where the evolution of the orientation along the deformation path, for given conditions of temperature and load, will be reported.

As previously stated, the decrease of $P_{200}^{x_3^c/X_1}$ with the draw ratio reflects the increasing orientation towards the stretching direction. Indeed, $P_{200}^{x_3^c/X_1}$ is well correlated with

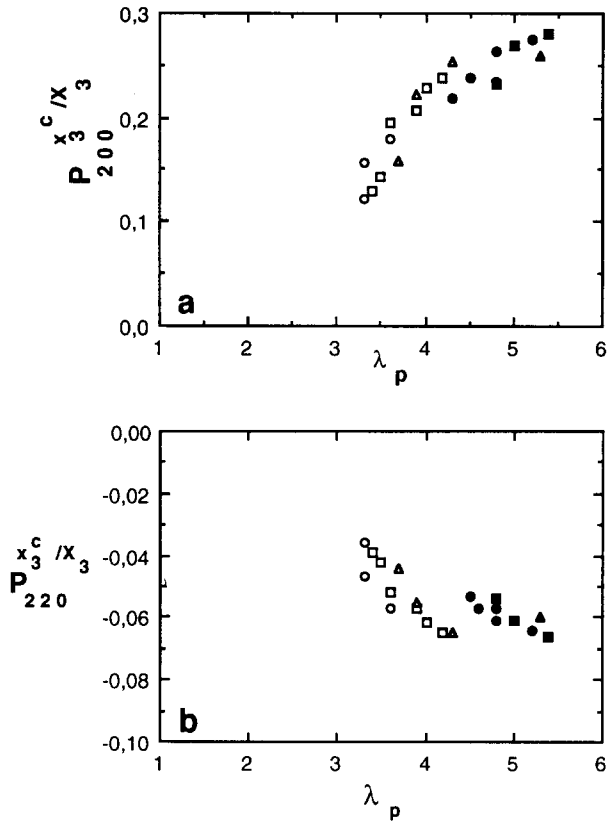

Figure 5 (a) $P_{200}^{x_3^c/X_3}$ and (b) $P_{220}^{x_3^c/X_3}$ plotted *versus* the plateau draw ratio for various temperatures (symbols as in *Figure 4*)

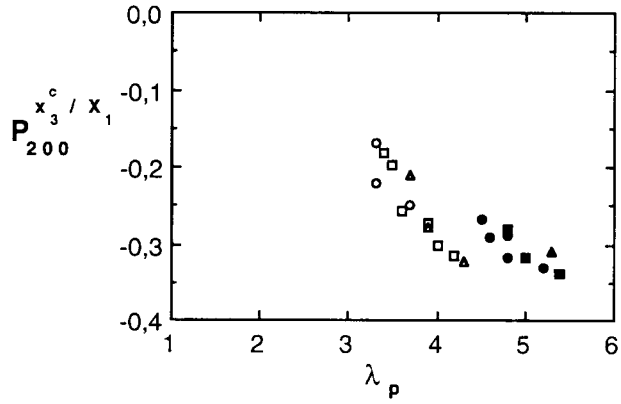

Figure 6 $P_{200}^{x_3^c/X_1}$ plotted *versus* the plateau draw ratio for various temperatures (symbols as in *Figure 4*)

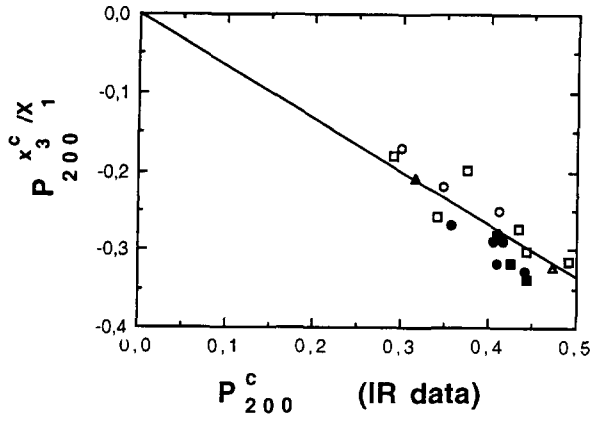

Figure 7 $P_{200}^{x_c'/X_1}$ plotted *versus* the chain axis orientation as measured by infra-red dichroism, P_{200}^{c} (symbols as in *Figure 4*)

$P_{200}^{x_c'/X_1}$ (orientation of the chain axis with respect to the draw direction), which has been measured on the same samples by infra-red dichroism techniques[13], as shown in *Figure 7*. Moreover, the relaxation of the chain axis between 95 and 100°C, directly observed by infra-red spectroscopy[13], is also apparent here using a much easier technique.

CONCLUSIONS

This study shows that measurements of refractive indices are easy to make and are powerful tools to investigate orientational properties, even in biaxially oriented systems. In this paper, we have shown that, for PET, information about the orientation of the plane of the phenyl ring can be obtained for any symmetry of the deformation process. In the case of uniaxial and uniaxial planar conditions, orientation of the chain axis can also be evaluated.

This approach can be extended to any polymer which possesses a uniaxial symmetry of the refractive index tensor of the unit cell. It is necessary to measure the three principal refractive indices and not only the birefringence in the plane of the film. Of course, the interpretation of refractive index measurements requires a knowledge of the principal polarizabilities, which are not available for all polymers. However, it is likely that these data, even for new polymers, can now be computed more easily using molecular modelling, especially in the case of semirigid or rigid polymers, or at least for polymers having a restricted number of conformations.

ACKNOWLEDGEMENTS

The authors would like to express their gratitude to Professor I. M. Ward for sharing data obtained by his group and for fruitful discussions, and gratefully acknowledge Rhône-Poulenc films for providing a PhD fellowship to P. L.

REFERENCES

1 Ward, I. M. 'Structure and Properties of Oriented Polymers', Applied Science, London, 1975
2 Stein, R. S. *J. Polym. Sci.* 1958, **32**, 335
3 Stein, R. S. *J. Polym. Sci.* 1961, **50**, 339
4 White, J. L. and Spruiell, J. E. *Polym. Eng. Sci.* 1981, **21**, 859
5 White, J. L. *Pure Appl. Chem.* 1983, **55**, 765
6 Cakmak, M., Spruiell, J. E. and White, J. L. *Polym. Eng. Sci.* 1984, **24**, 1390
7 Cakmak, M., Spruiell, J. E. and White, J. L. *J. Polym. Eng.* 1986, **6**, 291
8 Jarvis, D. A., Hutchinson, I. J., Bower, D. I. and Ward, I. M. *Polymer* 1980, **21**, 41
9 Kashiwagi, K., Cunningham, A., Manuel, A. J. and Ward, I. M. *Polymer* 1973, **14**, 111
10 Bower, D. I., Jarvis, D. A. and Ward, I. M. *J. Polym. Sci., Polym. Phys. Edn* 1986, **24**, 1459
11 Lapersonne, P., Tassin, J. F., Monnerie, L. and Beautemps, J. *Polymer* 1991, **32**, 3331
12 Lapersonne, P., Bower, D. I. and Ward, I. M. *Polymer* 1992, **33**, 1266
13 Lapersonne, P., Bower, D. I. and Ward, I. M. *Polymer* 1992, **33**, 1277
14 Daubeny, R., Bunn, C. W. and Brown, C. J. *Proc. R. Soc., London* 1954, **226**, 531
15 Ward, I. M. *Adv. Polym. Sci.* 1985, **66**, 81
16 Hutchinson, I. J., Ward, I. M., Willis, H. A. and Zichy, V. *Polymer* 1980, **21**, 55
17 Kaito, A., Nakayama, K. and Kenetsuna, H. *J. Polym. Sci., Polym. Phys. Edn* 1988, **26**, 1439
18 Cunningham, A., Ward, I. M., Willis, H. A. and Zichy, V. *Polymer* 1974, **15**, 749
19 Ward, I. M. and Wilding, M. A. *Polymer* 1977, **18**, 327
20 Long, S. PhD Thesis, University of Leeds, 1990
21 Spiby, P. PhD Thesis, University of Leeds, 1988
22 Le Bourvellec, G., Beautemps, J. and Jarry, J. P. *J. Appl. Polym. Sci.* 1990, **39**, 319
23 Le Bourvellec, G. and Beautemps, J. *J. Appl. Polym. Sci.* 1990, **39**, 329